# Effective thermal conductivity of loose particulate systems

B. O. ADUDA
*Physics Department, University of Nairobi, P. O. Box 30197 Nairobi Kenya*

The effective thermal conductivity for several loose particulate insulation systems has been measured in the temperature range from 273 K–900 K and the results compared to those predicted from three different models. The measured thermal conductivities increase with temperature. This is accounted for in terms of increased conduction by the fluid (air) and the radiative heat transfer through the media although the latter mode of heat transfer is relatively suppressed in materials containing finer particles. The model due to Zumbrunnen *et al.* [1] was found to predict values that closely agreed with the experimental values.

## 1. Introduction

In problems and applications involving heat transfer thermal conductivity is an important parameter. The diversity of such problems, materials and applications accounts for the numerous theoretical and experimental studies of thermal conductivity [1–13]. For example, high performance insulation for buildings, cold storage, furnaces etc. all depend on the heat transfer characteristics of the media used, and hence the need to know or predict their thermal conductivity. Since many materials are heterogeneous and complex, and since only their overall response to an applied temperature gradient is required, the macroscopic (effective) rather than the microscopic thermal conductivity is often measured. In porous and granular systems, the subject of this study, the effective thermal conductivity is a function of many parameters, amongst which are temperature, particle size distribution, porosity and pore size (distribution), type of fluid contained in the pores, the gas pressure, and thermal conductivities of the solid and fluid phases.

Numerous and diverse theoretical models [1, 3, 4, 6, 8–13] for calculating the effective thermal conductivity of heterogeneous (two-phase) media exist. It has however, been noted [3] that for porous systems not all the models are applicable in the entire porosity range and/or wide temperature range. A number of the models also do not take into account the contribution of radiative heat transfer to the effective thermal conductivity. In this study, the thermal conductivity of various loose-fill thermal insulation materials used to insulate institutional and domestic cooking stoves at the Bellerive Centre, Nairobi Kenya, have been measured from about 0 °C to about 630 °C. These cooking stoves, because of their efficiency and low wood-fuel or charcoal consumption, are gaining increased acceptance in many developing countries where biomass fuels are fast becoming scarce and expensive. The experimental results have been compared with those obtained from the theoretical models of Zumbrunnen *et al.* [1], Verma *et al.* [11] and Furmanski [8].

## 2. Experimental procedure

The materials; commercial vermiculite grade 4, clayworks brick powder (Clayworks Ltd.), black pottery and white pottery clay (both from Maragua, Central Kenya), swamp clay (from Thika) and red ant-hill soil (from Ruiru), hereafter designated VG4, BP, BPC, WPC, SC, and RAHS respectively were supplied by the Bellerive Centre, Nairobi.

The test samples, except for the vermiculite which was tested as supplied, were first sieved through sieve BSS No.7 (nominal aperture size ≈ 2411 μm) to remove any larger particles or organic matter. Black pottery clay whose particles were rather large was first crushed before sieving. This procedure of sample preparation was similar to that adopted by the supplier before using the materials as thermal insulators.

Thermal conductivity was measured using a thermal probe [14, 15]. Briefly, it consists of a cylindrical probe containing a heater wire surrounded by an infinite medium (large compared to the probe size) whose thermal properties is to be measured. When the conductor is heated at a rate **Q**, per unit length, an axially symmetric temperature field is set up in the medium. The rate of temperature change in the medium will depend on its thermal properties. Blackwell [14] has shown that the thermal properties of the medium can be determined from the relation

$$\Delta T(t) = T(t) - T_0 = A\ln(t) + C \qquad (1)$$

where $T(t)$ is the temperature at time $t$, $T_0$ is the initial temperature, $A$, and $C$ are constants. The constant $A$ is expressed as

$$A = Q(4\pi K)^{-1} \qquad (2)$$

0022–2461 

and is the slope of the $\Delta T(t)$ versus $\ln(t)$ plot, where $K$ is the thermal conductivity. $K$ is thus determined once $Q$ and $A$ are known.

In a typical test the granular sample (previously dried in an oven at 383 K for 24 h) was poured into a steel container, tapped lightly and sealed. The probe (length: diameter ratio $\cong 57:1$) was inserted centrally into the sample through a hole in the lid of the container. Thereafter the setup was placed inside an electric furnace/cooler and the heat input ($Q$) was supplied to the probe at a chosen temperature after equilibration ($\pm 1$ K). An iron–constantan thermocouple located close to the probe surface, and connected to a multi channel digital thermometer detected the temperature changes which were recorded every 10 s for a total period of 600 s. The linear portion of the graph of $\Delta T(t)$ versus $\ln(t)$ was used to determine $A$ and hence $K$. By setting the furnace/cooler at suitable temperatures and allowing for the steady state conditions to be achieved, thermal conductivities of the samples were determined at different temperatures. The temperature at a point in the sample near to the outer boundary was found to remain constant during the entire test period (600 s). This indicated that the temperatures recorded at the point close to the probe were not influenced by heat reflected from the inner walls of the container.

## 3. Heat transfer models

The prediction of effective thermal conductivities of granular beds has been attempted using various models of varying complexities. We will consider only a few that have been derived based on different assumptions, that are simple to use and/or are claimed to be improvements upon previous ones based on similar assumptions and are applicable over a wider porosity range.

### 3.1. The model of Zumbrunnen *et al.* [1]

This is a resistor model in which the heat flux is assumed to be linear and the different phases encountered are considered as thermal resistors obeying Ohm's law. It is further assumed that; (I) the pores are randomly distributed and are sufficiently small to exclude the convective heat transfer, (II) that the pore surfaces are grey, (III) the gas in the pores is radiatively nonparticipating, and (IV) that the solid material is opaque to radiation. The conduction through the fluid in the pores is catered for by using an adjustable dimensionless parameter $\mu$, that relates conduction across the pores to the conductivity of the solid phase. It is expressed as the ratio of the effective conduction length across a characteristic pore to the characteristic pore size.

The complex nature of the porous systems is simplified by use of geometric parameters to define a unit cell probability that allows the local heat transfer mechanisms to be derived. The advantages of this model are that the geometry of the pores is not required, and it is applicable over a wide range of porosity and temperature. With these assumptions Zumbrunnen *et al.* [1] obtained the following expression for effective thermal conductivity ($K_e$) for a porous solid of porosity ($\phi$) and characteristic pore size ($v$) with $K_s$ being the conductivity of the solid and $K_f$ the conductivity of the fluid.

$$K_e = \{\chi + \Gamma(\beta + 1)/\beta\} \{k_s^{-1}(\Gamma\Psi\beta^{-1} + \chi) + (1 + \Gamma)[v h_{rv} + k_f \mu^{-1}]^{-1}\}^{-1} \quad (3)$$

where

$$\chi = (1 + \beta)[(2 + \beta)(1 + \beta)^{-1}\ln(1 + \beta) + 1] / \beta\ln(1 + \beta) \quad (4)$$

$$\beta = \phi^{1/3}(1 - \phi^{1/3})^{-1} \quad (5)$$

$$\Gamma = 1 + \{\ln[(\beta + 1)/\beta]\}^{-1} \quad (6)$$

and $\Psi = 1$ for solids with closed pores and $\Psi = 0$ for solids with open (interconnected) pores. Here $\chi$ and $\Gamma$ define the expectation conduction lengths in the different paths in the direction of the heat flow as defined by the authors.

The radiative heat transfer coefficient across the pore is given as

$$h_{rv} = 4\sigma\varepsilon T^3 \quad (7)$$

where $T$ is the average pore surface temperature, $\varepsilon$ is the emissivity and has a value between 0–1, and $\sigma$ is the Stefan–Boltzmann constant equal to $5.735 \times 10^{-8}$ $\mathrm{J m^{-2} K^{-4} s^{-1}}$.

In order to apply Equation 3 to calculate $K_e$, we adopted the following procedures: (1) For each material a value $\mu$ was first obtained in the low temperature range where radiative heat transfer is negligible (as recommended by Zumbrunnen *et al.*). This value of $\mu$ was then retained for the entire range of temperatures. (2) The characteristic pore size ($v$) was estimated according to $v = 0.46d$ as suggested by Bhattacharya [16] where $d$ is the characteristic (mean) particle size. (3) The approximate emissivity ($\varepsilon$) values were obtained from literature [17], (4) $\Psi = 0$ when the pores were interconnected.

### 3.2. The model of Furmanski [8]

This is a model derived using the ensemble averaging technique to formulate the macroscopic heat transfer in the heterogeneous media. The assumptions are: (1) conduction is the only mode of heat transfer in the medium, (2) the microgeometry of the medium is time invariant, (3) the heterogeneous medium is a two component material containing spherical inclusions of thermal conductivity $k_i$ distributed chaotically in a matrix of thermal conductivity $k_m$. A characteristic length ($\imath$), also called the microdimension, of the heterogeneous medium is defined and it is the distance between inclusions in a periodic structure, or the grain/pore size in polycrystalline/granular materials. In the case of spherical inclusions of radius $R$, $\imath = R/v_i^{1/3}$ where $v_i$ is the volume fraction of the spheres. $\imath$ is related to the variation of local thermal conductivity. With these assumptions the expression for effective thermal conductivity could be written

$$K_e/k_m = 1 + \sigma'(v_i + F)\{1 + \sigma'(1 - v_i) + F\}^{-1} \quad (8)$$

where $\sigma' = (k_i - k_m)/k_m$, and $F$ is a function that depends on $\imath$, $\sigma'$, $v_i$ and the thermal wave vector ($k$) (cf. Equation 41 of Furmanski). The modulus of $k = 2\pi\Lambda^{-1}$, where $\Lambda$ is the thermal wavelength. In the limit of $\imath/\Lambda \to 0$, $K_e$ tends to maximum values, while for the special case of $\imath/\Lambda \to \infty$ the effective thermal conductivity tends to the limit given as

$$K_e/k_m = [v_i/\delta + (1 - v_i)]^{-1} \quad (9)$$

where $\delta = k_i/k_m$.

In this study, Equation 9, the simplified form of Furmanski's equation, and an added heat radiation term, $4v\sigma\varepsilon T^3$, assuming the conduction and radiation conductivities are independent [2, 4] was used to calculate $K_e$.

## 3.3. The model of Verma *et al.* [11]

This model, like that of Zumbrunnen *et al.* [1], is also a resistor model with the following assumptions: (1) the inclusions are spherical and homogeneously distributed in the mixture, (2) there is no contact thermal resistance between the solid and fluid phases of thermal conductivities $k_s$ and $k_f$ respectively, (3) radiative and convective heat transfers are neglected, (4) the heat flux is unidirectional. (Note that heat flux lines bend away from the pores if $k_f < k_s$, and towards the pore if $k_f > k_s$). The effective thermal conductivity is thus;

$$K_e = \frac{k_f\{2.5985F_p^{1/3}(k_s - k_f) + 3.224F_p^{-1/3}k_f\}}{(1 - 1.2407F_p^{1/3})\{2.5985F_p^{1/3}(k_s - k_f) + 3.224F_p^{-1/3}k_f\} + k_f} \quad (10)$$

which further reduces to

$$K_e = \{1 + 1.2407F_p^{1/3}\}k_f \text{ for } k_s \gg k_f. \quad (11)$$

Here $F_p$ is a porosity correction term originally given by Verma *et al* as $F_p = \exp[-c_2\Psi(1 - \phi)^{2/3}]$, with $c_2 = 2.4$ or 4.5 for non-spherical particles or spherical particles respectively. $\Psi$ is the sphericity.

Misra *et al.* [17] and Singh *et al.* [10] however, have noted that in the porosity correction factor ($F_p$) as given above $c_2$ is not a function of sphericity, but is a function of the ratio $k_s/k_f$. Accordingly, Singh *et al.* [10] proposed a porosity correction term $F_p$ given as

$$F_p = \phi^{1/3}\{c_1 + c_2\log(k_s/k_f)\} \quad (12)$$

where $c_1 = 0.1667$ and $c_2 = 0.3570$ for $1 < k_s/k_f < 500$, and $c_1 = -0.3258$ and $c_2 = 0.3675$ for $1000 < k_s/k_f < 15000$. Since $50 < k_s/k_f < 400$ for the granular materials in our study, the simplified Equations 11 and 12 were used to calculate $K_e$.

## 3.4. Thermophysical data and other parameters used in the theoretical models

It is noted that in all of the three models considered above, a knowledge of $k_s$ and $k_f$, the conductivities of the solid and fluid (air) phases is required. Due to the dearth of information, $k_s$ was estimated from the chemical compositional analysis which indicate that the materials comprised $SiO_2$ and $Al_2O_3$ (for the clays) and $SiO_2$, MgO and $Al_2O_3$ (for vermiculite) as the major constituents. Fitzpatrick [19] has observed that in the majority of soils and clays, $SiO_2$ is predominantly quartz or mixed, and $Al_2O_3$ occurs mainly in crystalline form. Therefore the thermal conductivity data for crystalline $SiO_{2\parallel}$, crystalline $Al_2O_3$ and MgO at different temperatures taken from literature [2, 20] were used to calculate $k_s$ for the clays according to the relation [21]

$$k_s/k_{SiO_{2\parallel}} = 1 - \frac{v_{Al_2O_3}}{(1 - k_{Al_2O_3}/k_{SiO_{2\parallel}})^{-1} - (1 - v_{Al_2O_3})/3} \quad (13)$$

Here $k_{SiO_{2\parallel}}$ is the thermal conductivity of $SiO_2$ parallel to the $c$-axis, $k_{Al_2O_3}$ and $v_{Al_2O_3}$ are the thermal conductivity and volume fraction of $Al_2O_3$ respectively. In the case of vermiculite (considered here to comprise three phases), the expression due to Brailsford and Major [22] was used to calculate $k_s$.

The chemical analysis data for materials were obtained from the following sources: vermiculite [23], Red ant-hill soil and black pottery clay [24], white pottery clay (assumed to be kaolinite) [25], brick powder [25]. No chemical analysis data was available for swamp clay (SC), hence $k_s$ was not calculated for this material but the $k_s$ value reported by Pande and Chaudhary [5] for mud powder was used in the calculations at low temperatures.

The thermal conductivity data for the fluid phase (air) was obtained from the empirical relation given by Shrotriya [26]

$$k_f = 0.0237 + 6.41 \times 10^{-5}T \quad (14)$$

where $T$ is the temperature. It was noted that Equation 14 gave similar results to those obtained from the Tsederberg [27] expression

$$k_f = k_o(T/T_o)^n \quad (15)$$

where $T$ is the absolute temperature, $k_o$ is the thermal conductivity of gas (air) at $T_o = 273$ K and $n$ is a constant ($n = 0.82$ for air).

The adopted characteristic (mean) particles size (d) of the materials were as follows: VG4 (d = 3.3 mm), WPC (d = 0.23 mm), BPC (d = 0.1 mm), BP (d = 0.1 mm), RAHS (d = 0.2 mm).

## 4. Results and discussion

The densities ($Mg\,m^{-3}$) of the materials were as follows: vermiculite (VGE) $1.423 \pm 0.001$, brick powder (BP) $2.260 \pm 0.019$, white pottery clay (WPC) $2.260 \pm 0.019$, black pottery clay (BPC) $1.87 \pm 0.06$, swamp clay (SC) $2.000 \pm 0.025$, and red ant-hill soil (RAHS) $2.05 \pm 0.06$ respectively.

Tables I and II show the experimental temperature–thermal conductivity data of the materials. These results are plotted in Fig. 1 for comparison. The calculated values are shown in Tables III–VIII. (In Tables III–VIII, the bracketed values were obtained from the Furmanski/Verma *et al.* equations with the radiation term added). The experimental and predicted results are compared in Figs 2–6.

It is noted (Fig. 1) that $K_e$ for all these granular systems increases with an increase in the temperature such that the curves mostly face upwards. This is indicative of the strong influence of conduction through the fluid phase and radiative heat transfer. These modes of heat transfer were noted to be greatest for VG4 ($\phi = 0.91$, $v = 1.518 \times 10^{-3}$m), WPC ($\phi = 0.538$, $v = 1.058 \times 10^{-4}$ m) and BP ($\phi = 0.448$, $v = 4.6 \times 10^{-5}$ m). This is consistent with the fact that the radiative heat transfer which can be considered as equivalent to an additional conduction term enhances the overall thermal conductivity. This contribution increases with increasing pore size [4, 28] and this explains why vermiculite and white pottery clay which have larger characteristic pore sizes respectively have the highest and second highest rate of change of $dK_e/dT$ of all the materials.

TABLE I Measured conductivity for brick powder (BP), White pottery clay (WPC) and red ant-hill soil (RAHS)

| Temperature (K) | Effective thermal conductivity ($Wm^{-1}K^{-1}$) BP ($\phi = 0.448$) | WPC ($\phi = 0.538$) | RAHS ($\phi = 0.527$) |
|---|---|---|---|
| 302.0 | 0.0732 | | |
| 305.0 | | | 0.0622 |
| 306.0 | | 0.0950 | |
| 426.0 | | 0.1165 | 0.0649 |
| 461.0 | 0.0888 | | |
| 508.0 | 0.0980 | | |
| 551.0 | | 0.1283 | |
| 561.0 | 0.0995 | | |
| 598.0 | | | 0.0653 |
| 714.0 | | 0.1647 | |
| 715.0 | 0.1275 | | |
| 735.0 | | | 0.0743 |
| 803.0 | | 0.1922 | |
| 821.0 | 0.1430 | | |
| 868.0 | | | 0.0805 |

TABLE II Measured conductivity for black pottery clay (BPC), swamp clay (SC) and vermiculite grade 4 (VG4)

| Temperature (K) | Effective thermal conductivity ($Wm^{-1}K^{-1}$) BPC ($\phi = 0.402$) | SC ($\phi = 0.554$) | VG4 ($\phi = 0.91$) |
|---|---|---|---|
| 278.0 | | | 0.0219 |
| 285.0 | | | 0.0227 |
| 304.0 | 0.0788 | | |
| 306.0 | | | 0.0249 |
| 307.0 | | 0.0556 | |
| 320.0 | 0.0798 | | |
| 324.0 | | | 0.0257 |
| 357.0 | | | 0.0385 |
| 375.0 | | | 0.0428 |
| 406.0 | | 0.0597 | |
| 425.0 | | | 0.0542 |
| 521.0 | 0.0878 | | |
| 527.0 | | | 0.1070 |
| 621.0 | 0.0948 | 0.0680 | |
| 714.0 | | 0.0738 | |
| 760.0 | | | 0.2147 |
| 798.0 | 0.1066 | | |
| 829.0 | 0.1099 | | |
| 841.0 | | | 0.2401 |
| 880.0 | | 0.0836 | |
| 905.0 | | | 0.3251 |

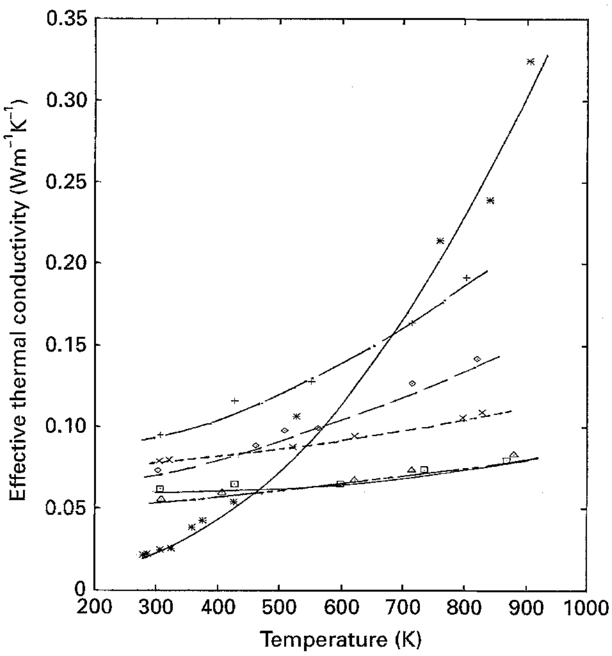


*Figure 1* Measured thermal conductivities for; (◇) brick powder (BP), (+) White pottery clay (WPC), (⊡) red ant-hill soil (RAHS), (△) swamp clay (SC), (×) black pottery clay (BPC) and (*) vermiculite grade 4 (VG4).

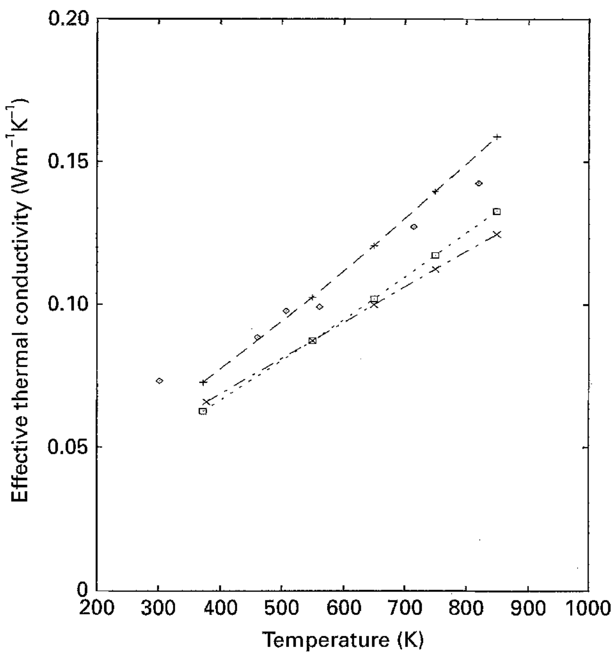


*Figure 2* (◇) Experimental ('BP') and predicted thermal conductivity of brick powder. The models used in the analysis were those of; (+) Zumbrunnen *et al.* [1], (⊡) Furmanski [8] and (*) Verma *et al.* [11].

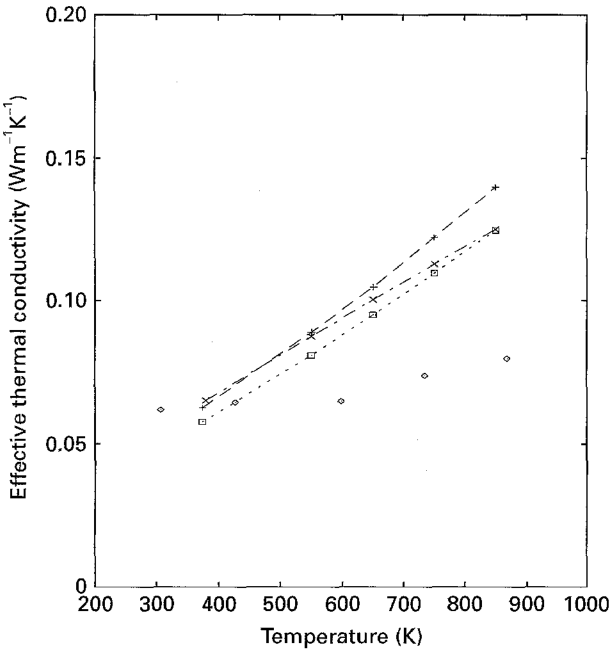


*Figure 3* (◇) Experimental ('RAHS') and predicted thermal conductivity of red ant-hill soil. The models used and the data points calculated using these models are represented by the same symbols as in Fig. 2.

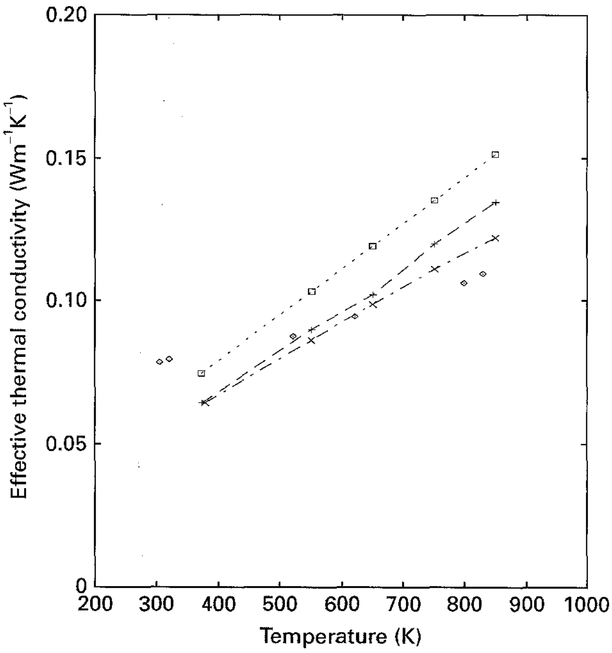


*Figure 5* (◇) Experimental ('BPC') and predicted thermal conductivity of black pottery clay. The models used and the data points calculated using these models are represented by the same symbols as in Fig. 2.

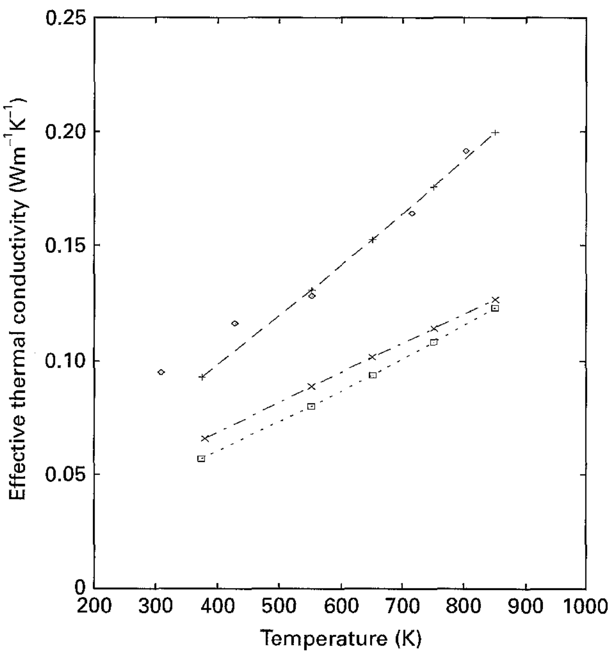


*Figure 4* (◇) Experimental ('WPC') and predicted thermal conductivity of white pottery clay. The models used and the data points calculated using these models are represented by the same symbols as in Fig. 2.

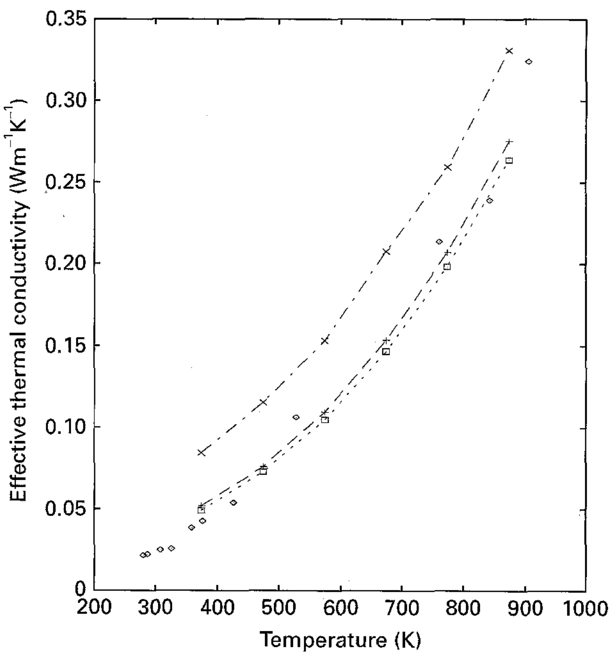


*Figure 6* (◇) Experimental ('VG4') and predicted thermal conductivity of vermiculite grade 4. The models used and the data points calculated using these models are represented by the same symbols as in Fig. 2.

Above 473 K, SC ($\phi = 0.554$) and RAHS ($\phi = 0.527$) are seen to have the lowest and nearly equal thermal conductivities over the temperature range. Further, the rate at which their $K_e$ increase with temperature is rather small. The low $K_e$ values of these two materials are corroborated by their low $K_s$ and high porosity values. It is further postulated that these materials probably contained higher organic matter (humus) content [24] which contributed to their low $K_s$. The organic matter would burn out or volatilize to produce ash/extra voids with even lower thermal conductivity. This postulation may also explain the observed large deviation between experimental and theoretical values (Fig. 3) for RAHS particularly at high temperatures, where owing to the small characteristic pore sizes of these materials radiative heat transfer is greatly inhibited.

The $K_e$ for WPC ($\phi = 0.538$)) is noted (Fig. 1) to be greater than $K_e$ of BP ($\phi = 0.448$) at all temperatures contrary to expectations at low temperatures.

A plausible explanation for this result is the role played by the contact resistance due to microroughness and/or inhomogeneities at the particle–particle contact points. It has been reported [9, 13, 29] that $K_e$ in granular systems is very sensitive to the nature of particle–particle contact at large values of the ratio $\delta = k_s/k_f$. Litovsky and Shapiro [29] have noted that these inhomogeneities, although they contribute significantly to the thermal resistance, only contribute insignificantly to the total porosity.

When the experimental results and theoretical values of $K_e$ are compared (Figs 2–6), it is observed that at lower temperature ranges (T < 573 K), all the models give results that compare reasonably well with the experimental values. An exception is WPC for which the models of Furmanski [8] and Verma *et al.* [11] tend to underestimate $k_s$. Note that in Figs 2–6, a Furmanski equation with an added radiative term has been used, while the expression of Verma *et al.* with an extra radiation term has been used in Fig. 6. Above 573 K, deviations, the magnitude of which is material and model dependent, between theoretical and experimental values are noted to occur. For example, all the models overestimate $K_e$ for RAHS (Fig. 3) and BPC (Fig. 5). On the other hand the expressions of Furmanski and Verma *et al.* underestimate $K_e$ for BP (Fig. 2), and WPC (Fig. 4). Without the radiation term, the model of Verma *et al.* grossly underestimates the $K_e$ values of vermiculite but with the radiation term, it overestimates it. For this material the models

TABLE III Calculated thermal conductivity for brick powder

| Temperature (K) | $\mu$ | $\varepsilon$ | $F_p$ | $k_s$ | Thermal conductivity ($Wm^{-1}K^{-1}$) Equation 3 | Equation 9 | Equation 11 |
|---|---|---|---|---|---|---|---|
| 373 | 0.68 | 0.93 | 0.88 | 13.97 | 0.0727 | 0.0615 (0.0625) | 0.0659 |
| 550 | 0.68 | 0.91 | 0.72 | 5.33 | 0.1028 | 0.0844 (0.0876) | 0.0876 |
| 650 | 0.68 | 0.89 | 0.69 | 4.53 | 0.1209 | 0.0971 (0.1023) | 0.1003 |
| 750 | 0.68 | 0.87 | 0.65 | 3.94 | 0.1398 | 0.1097 (0.1175) | 0.1127 |
| 850 | 0.68 | 0.85 | 0.63 | 3.49 | 0.1595 | 0.1222 (0.1332) | 0.1251 |

TABLE IV Calculated conductivity for red ant-hill soil

| Temperature (K) | $\mu$ | $\varepsilon$ | $F_p$ | $k_s$ | Thermal conductivity ($Wm^{-1}K^{-1}$) Equation 3 | Equation 9 | Equation 11 |
|---|---|---|---|---|---|---|---|
| 373 | 0.75 | 0.91 | 0.85 | 9.07 | 0.0630 | 0.0569 (0.0579) | 0.0655 |
| 550 | 0.75 | 0.90 | 0.73 | 4.89 | 0.0894 | 0.0782 (0.0815) | 0.0879 |
| 650 | 0.75 | 0.90 | 0.70 | 4.20 | 0.1050 | 0.0900 (0.0954) | 0.1006 |
| 750 | 0.75 | 0.89 | 0.66 | 3.69 | 0.1225 | 0.1017 (0.1099) | 0.1131 |
| 850 | 0.75 | 0.89 | 0.64 | 3.31 | 0.1406 | 0.1133 (0.1252) | 0.1255 |

TABLE V Calculated conductivity for white pottery clay

| Temperature (K) | $\mu$ | $\varepsilon$ | $F_p$ | $k_s$ | Thermal conductivity ($Wm^{-1}K^{-1}$) Equation 3 | Equation 9 | Equation 11 |
|---|---|---|---|---|---|---|---|
| 373 | 0.50 | 0.91 | 0.88 | 11.17 | 0.0929 | 0.0558 (0.0570) | 0.0659 |
| 550 | 0.50 | 0.88 | 0.78 | 7.47 | 0.1307 | 0.0768 (0.0804) | 0.0891 |
| 650 | 0.50 | 0.84 | 0.75 | 6.20 | 0.1529 | 0.0884 (0.0940) | 0.1019 |
| 750 | 0.50 | 0.82 | 0.71 | 5.29 | 0.1764 | 0.1000 (0.1086) | 0.1145 |
| 850 | 0.50 | 0.75 | 0.68 | 4.60 | 0.2003 | 0.1116 (0.1235) | 0.1270 |

TABLE VI Calculated conductivity for black pottery clay

| Temperature (K) | μ | ε | $F_p$ | $k_s$ | Thermal conductivity ($Wm^{-1}K^{-1}$) Equation 3 | Equation 9 | Equation 11 |
|---|---|---|---|---|---|---|---|
| 373 | 0.85 | 0.86 | 0.79 | 10.01 | 0.0645 | 0.0745 (0.0750) | 0.0646 |
| 550 | 0.85 | 0.83 | 0.67 | 5.12 | 0.0902 | 0.1020 (0.1035) | 0.0866 |
| 650 | 0.85 | 0.80 | 0.64 | 4.37 | 0.1024 | 0.1172 (0.1195) | 0.0991 |
| 750 | 0.85 | 0.78 | 0.61 | 3.82 | 0.1202 | 0.1323 (0.1358) | 0.1114 |
| 850 | 0.85 | 0.75 | 0.58 | 3.40 | 0.1352 | 0.1471 (0.1520) | 0.1226 |

TABLE VII Calculated conductivity for swamp clay

| Temperature (K) | μ | $F_p$ | Thermal conductivity ($Wm^{-1}K^{-1}$) $k_s$ | Equation 3 | Equation 9 | Equation 11 |
|---|---|---|---|---|---|---|
| 309 | 0.70 | 0.82 | 5.7 | 0.0552 | 0.0476 | 0.0562 |

TABLE VIII Calculated conductivity for vermiculite grade 4

| Temperature (K) | μ | ε | $F_p$ | Thermal conductivity ($Wm^{-1}K^{-1}$) $k_s$ | Equation 3 | Equation 9 | Equation 11 |
|---|---|---|---|---|---|---|---|
| 373.0 | 0.9 | 0.91 | 1.093 | 14.85 | 0.0520 | 0.0330 (0.0494) | 0.0686 (0.0850) |
| 473.0 | 0.9 | 0.90 | 1.062 | 11.75 | 0.0768 | 0.0401 (0.0733) | 0.0827 (0.1159) |
| 573.0 | 0.9 | 0.89 | 0.97 | 9.31 | 0.1103 | 0.0471 (0.1054) | 0.0956 (0.1539) |
| 673.0 | 0.9 | 0.88 | 0.92 | 7.77 | 0.1542 | 0.0541 (0.1475) | 0.1088 (0.2088) |
| 773.0 | 0.9 | 0.86 | 0.88 | 6.84 | 0.2084 | 0.0613 (0.1996) | 0.1353 (0.2604) |
| 873.0 | 0.9 | 0.85 | 0.85 | 6.03 | 0.2767 | 0.0683 (0.2652) | 0.1353 (0.3322) |

of Zumbrunnen *et al.* and Furmanski (with added radiation term) give results in excellent agreement with the experimental data. On the whole, the model of Zumbrunnen *et al.* when, compared to the two other models, gave results that were in better agreement with the experimental results for all the materials. This result emphasizes the limitation imposed by assuming inclusions to be spherically shaped as in the two other models considered above.

It worthy of note that the μ and $F_p$ parameters (Tables III–VIII), especially, at the low temperature ranges are quite close. This would tend to reinforce the fact that both these parameters depend on the ratio $k_s/k_f$. In this study μ was found to be in the range 0.5–0.9 compared to that of Zumbrunnen *et al.* [1] which ranged from 0.3–0.7. The $F_p$ values were in the range of 0.58–1.093 compared to the range of 0.3175–0.9035 reported by Verma *et al* [11].

## 5. Conclusions

The effective thermal conductivity of several loose-fill insulation materials has been measured and these results compared with those obtained from various theoretical models. An observed increase in $K_e$ with temperature was attributed to the enhanced conductive (mainly by the fluid phase) and radiative heat transfers in the granular porous media. The generally lower $K_e$ of BP compared that WPC was attributed to the possible presence of inhomogeneities, and microroughness which significantly affect thermal conductivity but minimally influence the overall porosity. The model of Zumbrunnen *et al.* [1] was found to give the best results over a wide porosity and temperature range. At low temperatures ( < 573 K) all the three considered models gave results that reasonably matched the experimental values.

## Acknowledgements

This work was supported by the Kenya Environmental Non-Governmental Organizations (KENGO). An associateship made possible by the generosity of the Swedish Agency for Research Cooperation with Developing Countries (SAREC) to, and the hospitality and use of facilities of, the International Centre for

Theoretical Physics (ICTP), Trieste, Italy are gratefully acknowledged.

## References


1. D. A. ZUMBRUNNEN, R. VISKANTA and F. P. INCROPERA, *Int. J. Heat Mass Transfer* **29** (1986) 275.
2. J. S. M. BOTTERILL, A. G. SALWAY and Y. YEOMAN, *Int. J. Heat Mass Transfer* **32** (1989) 595.
3. S. TORQUATO, *Rev. Chem. Engng* **4** (1987) 151.
4. A. S. WAGH, *J. Mater. Sci.* **28** (1993) 3715.
5. R. N. PANDE and D. R. CHAUDHARY, *Pramana* **23** (1984) 599.
6. R. N. PANDE, V. KUMAR and D. R. CHAUDHARY, *ibid* **22** (1984) 63.
7. G. V. SAMSONOV, (ed), "The Oxide Handbook", (IFI/Plenum, New York, 1973).
8. P. FURMANSKI, *Int. J. Heat Mass Transfer* **35** (1992) 3047.
9. G. K. BATCHELOR and R. W. O'BRIEN, *Proc. R. Soc. Lond.* **A.33 355** (1977) 313.
10. R. SINGH, K. J. SINGH and D. R. CHAUDHARY, *J. Phys. D: Appl. Phys.* **28** (1995) 1573.
11. L. S. VERMA, A. K. SHROTRIYA, R. SINGH and D. R. CHAUDHARY, *ibid* **24** (1991) 1729.
12. T. H. BAURER, *Int. J. Heat Mass Transfer* **36** (1993) 4181.
13. D. R. SHONNARD and S. WHITAKER, *ibid* **32** (1989) 503.
14. J. H. BLACKWELL, *J. Appl. Phys.* **25** (1954) 137.
15. J. J. HEALY, J. C. DE GROOT and J. KESTIN, *Physica B + C* **82** (1976) 392.
16. A. K. BHATTACHARYA, *J. Amer Ceram. Soc.* **74** (1991) 2113.
17. A. SALA, "Radiant Properties of Materials: Tables of radiant values for black body and real materials" (Elsevier, Amsterdam, 1986).
18. K. MISRA, A. K. SHROTRIYA, R. SINGH and D. R. CHAUDHARY, *J. Phys. D: Appl. Phys.* **27** (1994) 732.
19. E. A. FITZPATRICK, "SOILS Their Formation, classification and distribution" (Longmans, London, 1980) p. 20.
20. G. W. C. KAYE and T. H. LABY, "Table of Physical and Chemical Constants and some Mathematical Functions" 5th Edn (Longmans, London 1986).
21. A. V. LUIKOV, "Heat and Mass Transfer" (English Translation) (Mir Publishers, Moscow, 1980).
22. A. D. BRAILSFORD and K. G. MAJOR, *Brit. J. Appl. Phys.* **15** (1964) 313.
23. B. ADUDA, MSc Thesis Nairobi University, 1987.
24. R. KINYANJUI, MSc Thesis Egerton University, 1995.
25. F. NYONGESA, MSc Thesis Nairobi University, 1994.
26. A. K. SHROTRIYA, *Indian J. Pure and Appl. Phys.* **29** (1991) 339.
27. N. V. TSEDERBERG, "Thermal Conductivity of Gases and Liquids" (Translated by Scripta Massachusetts, D. Cess (ed) The MIT Press, Cambridge MA, 1965) p. 67.
28. A. J. HELTE, *Appl. Phys.* **73** (1993) 7167.
29. E. Y. LITOVSKY and M. SHAPIRO, *J. Amer Ceram. Soc.* **75** (1992) 3425.


*Received 13 November 1995*
*and accepted 18 March 1996*